

Exploiting Long-Term Dependencies for Generating Dynamic Scene Graphs

Shengyu Feng^{1*}Subarna Tripathi²Hesham Mostafa²Marcel Nassar²Somdeb Majumdar²¹University of Illinois at Urbana Champaign²Intel Labs

shengyu8@illinois.edu, {subarna.tripathi, hesham.mostafa, marcel.nassar, somdeb.majumdar}@intel.com

Abstract

Structured video representation in the form of dynamic scene graphs is an effective tool for several video understanding tasks. Compared to the task of scene graph generation from images, dynamic scene graph generation is more challenging due to the temporal dynamics of the scene and the inherent temporal fluctuations of predictions. We show that capturing long-term dependencies is the key to effective generation of dynamic scene graphs. We present the detect-track-recognize paradigm by constructing consistent long-term object tracklets from a video, followed by transformers to capture the dynamics of objects and visual relations. Experimental results demonstrate that our Dynamic Scene Graph Detection Transformer (DSG-DETR) outperforms state-of-the-art methods by a significant margin on the benchmark dataset Action Genome. We also perform ablation studies and validate the effectiveness of each component of the proposed approach.

1. Introduction

A scene graph is a directed graph where each node represents a labelled object and each edge represents an inter-object relationship, also known as a *predicate*. Grounded on this high-level semantic structure, scene graph generation (SGG) can be used to improve performance on downstream tasks such as image captioning [25, 2, 39, 38], visual question answering [13], image retrieval [17, 37, 30], image generation [16, 20, 35], and robotic manipulation planning [26]. Recent efforts in generating high-quality scene graphs from static images have led to notable breakthroughs due to the expressive representation of such graphs.

However, the task of dynamic scene graph generation from video is relatively new, more challenging, and presents several unsolved problems. The naive solution to this task is simply applying the static scene graph generation method on each video frame without considering temporal context. Recently a line of work [3, 6, 34] emerged that demonstrated the importance of capturing the spatial as well as the temporal

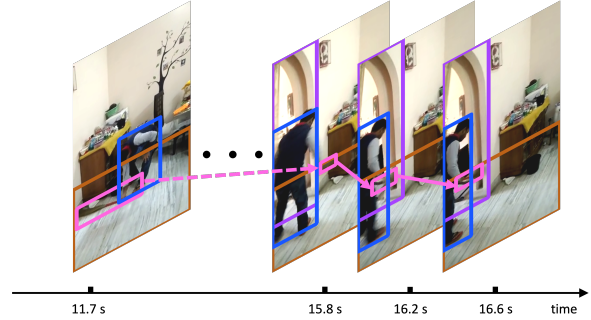


Figure 1: An example where the short-term temporal dependencies fail. The broom, bounded by the pink bounding boxes, is quite challenging to recognize on the rightmost three frames. Previous methods capturing only the short-term dependencies (indicated by the solid pink arrows) fail to make the correct prediction, while our method capturing the long-term dependencies (over a period of more than 4 seconds), can successfully recognize the broom and predict the human-broom relationships.

dependencies for dynamic scene graph generation tasks.

The predominant ways to realize spatio-temporal consistency focus on the construction of the spatio-temporal graph. Arnab *et al.* [3] constructed a unified graph structure, composed of a fully connected graph over the foreground nodes from the frames in a sliding window, and the connections between the foreground nodes and context nodes in each frame. Although this spatio-temporal graph can successfully perform message passing over both the spatial and temporal domains, such a fully connected graph is computationally expensive. In practice, such models use a small sliding window consisting of 3 to 5 key frames, making them incapable of reasoning over long-term sequences. Another recent work, Spatial-Temporal Transformer (STTran) [6] grounds the model on the adjacent key frames. As a result, these methods can only achieve short-term consistency and fail to capture long-term dependencies.

Fig 1 shows an example where occlusion and fast movement make it extremely difficult for any static image-based object detector to recognize the broom (bounded by the pink bounding box) in the three rightmost video frames. Any model that relies on capturing only short-term dependencies will fail to detect objects correctly in scenarios such as this example. This will

*Work partially done during an internship at Intel Labs.

result in incorrect dynamic scene graph generation. Predictions in frames where an object might be occluded may be improved by leveraging correct predictions from frames where it is easily detectable and recognizable. Since such “good” frames may be several frames in the past or the future (4 seconds in this example), capturing long-term dependencies is crucial to improve the overall scene graph generation performance.

In this paper, we study the benefits of utilizing long-term temporal dependencies for objects and relations in dynamic scene graph generation tasks. We quantify it via estimating the hypothetical best case by exploiting the ground-truth tracking information when evaluated on scene graph generation tasks using Recall metric. This hypothetical best case significantly outperforms existing methods on dynamic scene graph generation. Next, we propose a paradigm of detect-track-recognize for consistent video object detections. To this end, we construct the temporal sequences by tracking each object instance using the Hungarian matching algorithm [19], and apply a transformer encoder to leverage the temporal consistency for all such sequences. We also model the relationship transitions through the sequences of predicated subject-object classes using another transformer network. Our framework, named **DSG-DETR** (Dynamic Scene Graph Detection Transformer) performs comparably with the hypothetical best case explained above. The experimental results on the Action Genome dataset [15] also demonstrate that **DSG-DETR** can achieve significant improvements over the state-of-the-art methods for video scene graph generation.

The main contributions of our work can be summarized as:

- We hypothesize that the key to improving dynamic scene graph generation is in capturing *long-term* temporal dependencies of objects and visual relationships.
- We quantify the benefit of capturing long-term dependencies by estimating the hypothetical best case (an upper-bound) on the SGG task performances by utilizing the ground truth object tracks.
- We then show that by exploiting a tracking methodology which involves per-frame detections followed by temporally consistent object recognition, namely the detect-track-recognize paradigm, our method DSG-DETR approaches the hypothetical best case performance.
- DSG-DETR significantly outperforms existing state-of-the-art methods on the video scene graph generation benchmark dataset Action Genome.

2. Related work

Scene graph generation. Scene graphs are structured representation of images where object instances and inter-object relationships are encoded by nodes and edges in a graph, respectively. Scene graph generation has become an important problem in computer vision since Johnson *et al.* [17] introduced the concept of graph-based image representation. A large body of work

has focused on scene graph generation from images [40, 21, 33, 41, 24, 22]. These methods focus on either sophisticated architecture design or contextual feature fusion strategies, such as message passing or recurrent neural networks, to optimize SGG performance on the image scene graph benchmark dataset [18].

However, all these methods are limited to static images without any consideration of the dynamics of a video. Video scene graph generation is significantly more challenging than image scene graph generation due to the underlying spatio-temporal dynamics involving objects and inter-object relationships. A line of recent and concurrent work [3, 6, 34, 14] looks at the problem of video scene graph generation via modeling the spatio-temporal dynamics of relationships. While [3] takes an approach of message passing in a spatio-temporal graph for capturing the relationship dynamics, others rely on visual transformers for it.

Transformer models in video analysis. Following the immense success of transformers [36] in natural language processing, they have been shown to be effective for image perception tasks [7, 4, 27] and video understanding tasks [32, 9, 8]. A recent work studies transformers for video scene graph generation [6], which is also the focus of this paper. Another closely related problem is Human-Object-Interaction (HOI) detection from video where a Human-Object Relationship transformer has been applied [14] successfully.

We hypothesize and experimentally show that the temporal fluctuation of object-level predictions hinders the performance of dynamic SGG tasks. While [6] aims to capture only the relationship dynamics via spatial encoder and temporal decoder, temporally consistent object predictions largely remain unaddressed. To the best of our knowledge none of the methods aims to systematically capture the long-term dynamics at object-level as well as visual relationship level for dynamic SGG tasks. We use STTran [6] as our baseline and build our model atop it. To summarize, we utilize a detect-track-recognize paradigm where tracks are formed from the frame-level detections over all key frames in a video. Next, an object-centric transformer is employed on these sequences resulting in temporally consistent object recognition, followed by a spatio-temporal relationship transformer on the predicted sequences of the same subject-object classes. They boost the performance over the baseline significantly.

3. Problem statement and notations

In this section, we clarify the notations used in this paper and make a formal definition of the problem we study. We also detail the preliminaries of the transformer model.

3.1. Dynamic scene graph generation

Given a video as a sequence of I key frames, we want to predict the objects for each frame, in terms of their positions and classes, and the relationships among them. Use \mathcal{C} and \mathcal{P} to denote the object class set and the predicate set respectively.

We define each object as a tuple comprising its bounding box \mathbf{b} and object class \mathbf{c} , i.e., $\mathcal{O} = \langle \mathbf{b}, \mathbf{c} \rangle$. Here, $\mathbf{b} \in [0, 1]^4$ is a vector composed of the object center coordinates and its width and height relative to the image size. $\mathbf{c} \in \{0, 1\}^{|\mathcal{C}|}$ is a one-hot vector with $\mathbf{c}[i] = 1$ and all other dimensions 0, where the i -th element of \mathcal{C} corresponds to the class of this object.

The relationship tuple for a subject-object pair is defined as $\langle \mathcal{O}_s, p, \mathcal{O}_o \rangle$, which correspond to the subject, predicate and object respectively, and $p \in \mathcal{P}$. There could be multiple relationships for a subject-object pair and we represent these predicates as a vector $\mathbf{p} \in \{0, 1\}^{|\mathcal{P}|}$, where $\mathbf{p}[i] = 1$ indicates the appearance of the i -th predicate in \mathcal{P} and the corresponding relationship triplet $\langle \mathcal{O}_s, \mathcal{P}_i, \mathcal{O}_o \rangle$.

Furthermore, we denote the distributions of the classes and predicates as $\tilde{\mathbf{c}} \in [0, 1]^{|\mathcal{C}|}$ and $\tilde{\mathbf{p}} \in [0, 1]^{|\mathcal{P}|}$, where $\sum_i \tilde{\mathbf{c}}[i] = 1$.

3.2. Transformer

Transformers [36] are a powerful tool for sequence modeling. In this work, we only use a transformer encoder, each layer of which consists of the Multi-Head Self Attention (MSA) module, layer normalization (LN) and a feedforward network (FFN). Note that the attention operation over the queries $\mathbf{Q} \in \mathbb{R}^{n \times d_q}$, keys $\mathbf{K} \in \mathbb{R}^{n \times d_k}$ and values $\mathbf{V} \in \mathbb{R}^{n \times d_v}$, where $d_q = d_k$, is defined as

$$\text{Attention}(\mathbf{Q}, \mathbf{K}, \mathbf{V}) = \text{Softmax}\left(\frac{\mathbf{Q}\mathbf{K}^T}{\sqrt{d_k}}\right)\mathbf{V}. \quad (1)$$

In self attention, the queries, keys and values are the linear projections of the input $\mathbf{X} \in \mathbb{R}^{n \times d}$ with $\mathbf{Q} = \mathbf{X}\mathbf{W}^Q$, $\mathbf{K} = \mathbf{X}\mathbf{W}^K$, $\mathbf{V} = \mathbf{X}\mathbf{W}^V$, where $\mathbf{W}^Q, \mathbf{W}^K, \mathbf{W}^V \in \mathbb{R}^{d \times d}$ and $d_q = d_k = d_v = d$. The MSA uses different weights for the projections and obtains different attention heads, which can be written as

$$\text{MSA}(\mathbf{X}) = \text{Concat}(\text{head}_1, \dots, \text{head}_h)\mathbf{W}^O \quad (2)$$

$$\text{head}_i = \text{Attention}(\mathbf{X}\mathbf{W}_i^Q, \mathbf{X}\mathbf{W}_i^K, \mathbf{X}\mathbf{W}_i^V), \quad (3)$$

where $\mathbf{W}^O \in \mathbb{R}^{d \times d_{\text{model}}}$. For each transformer encoder layer, its structure is defined as

$$\mathbf{Y} = \text{LN}(\text{MSA}(\mathbf{X}) + \mathbf{X}) \quad (4)$$

$$\text{EncoderLayer}(\mathbf{X}) = \text{LN}(\text{FFN}(\mathbf{Y}) + \mathbf{Y}). \quad (5)$$

Let $\mathbf{H}_0 = \mathbf{X}$, the output of an l -layer transformer encoder can be formulated as

$$\mathbf{H}_i = \text{EncoderLayer}(\mathbf{H}_{i-1}), 1 \leq i \leq l \quad (6)$$

$$\text{Encoder}(\mathbf{X}) = \mathbf{H}_l. \quad (7)$$

If the sequence order matters, an additional positional encoding $PE(\mathbf{X})$ can be added to \mathbf{X} at the input, i.e., $\text{Encoder}(\mathbf{X} + PE(\mathbf{X}))$. In this paper, we use the sinusoidal encoding from the original transformer [36].

4. Methodology

In this section, we first identify the main challenges in modeling the temporal dynamics, then we discuss how DSG-DETR addresses them.

4.1. Temporal dynamics

The generation of dynamic scene graphs relies on reasoning over both spatial and temporal information. However, existing literature lacks a methodical analysis on what kind of information is needed for the temporal and spatial consistencies. In our experiments, we find the following aspects the main challenges for dynamic scene graph generation,

Temporal object consistency. Static image based object detectors fail to detect video objects consistently due to the inherent motion blur, fast movement, occlusion and inherent temporal variation of predictions. Challenging cases like severe occlusion pose great difficulty in identifying an object from a single frame. We show that grounding the predictions over a long-term temporal context and enforcing it to be temporally consistent - i.e., avoiding sudden appearances or disappearances of object representations - results in more accurate and consistent object detections in video.

Temporal relationship transition. Besides the temporal object consistency, the other challenge for dynamic scene graph generation is the temporal relation transition. Here we use the phrase *transition* rather than *consistency* since we do not want the relationships to be the same across all frames as the objects move and their relationships change over time. We aim to maximize the conditional probability of a relationship given the previous relationships and the current observation.

For the remaining part of this section, we describe how we circumvent these issues separately. Fig 2 describes the overall framework of DSG-DETR, which consists of an object transformer and a spatio-temporal relationship transformer, dealing with the object consistency and relationship transition respectively.

4.2. Temporal object consistency

4.2.1 Constructing tracking sequences

Unlike [3] that connects all objects in neighboring frames in a sliding window fashion, we only connect the objects which exhibit *apparent* similarity in either the visual feature or the spatial location. Our relatively sparser connections allow us to reason over long-term temporal contexts for a given computational and memory budget. To this end, we ground our method on a coarse tracking algorithm. It's worth noting that although our method is based on tracking, we do not strictly require the correct alignment among the objects. The purpose of our tracking is to group the most relevant features in the frames for an efficient message passing.

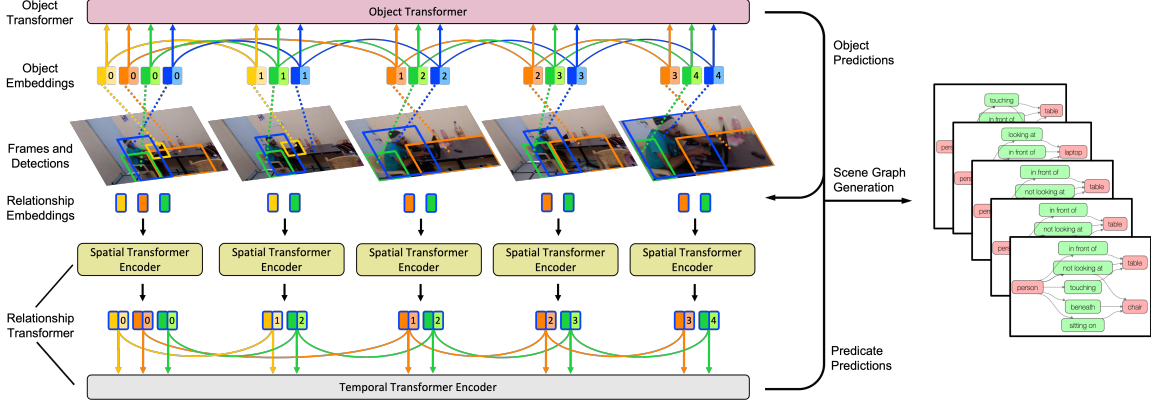


Figure 2: Visualization of the DSG-DETR model. The upper half visualizes the object transformer and the lower half sketches the relationship transformer. Each color (orange, tangerine, green and blue) corresponds to one object. The token boxes without borderline represent object embeddings, and those with the borderline represent relationship embeddings, where the colors of the borderline and token box indicate the subject and object respectively. The token boxes with numbers inside are the positional encoding, e.g., the blue box with “1” inside denotes its position in the blue tracklet. The solid lines connecting the token boxes stand for the tracking results.

Prior to the construction of the tracking sequences, we pass all the frames in the video to Faster R-CNN [28] to obtain the object bounding boxes (if not available), object class distributions and object features. In the following text, we use the definition of detection as $\langle \mathbf{b}, \tilde{\mathbf{c}}, \mathbf{f} \rangle$, where \mathbf{b} and $\tilde{\mathbf{c}}$ correspond to the bounding box and class distribution respectively and $\mathbf{f} \in \mathbb{R}^{2048}$ is the visual feature vector of the bounding box from Faster R-CNN.

Starting from the first frame, we iteratively match the detections with previous tracklets [10], where the tracking could be treated as a mapping $\sigma(\cdot, \cdot): \mathbb{Z}^+ \times \mathbb{Z}^+ \rightarrow \mathbb{Z}^+$. Here $\sigma(i, j)$ assigns the j -th detection in the i -th frame to $\sigma(i, j)$ -th tracklet. Specifically, we denote the tracking result for the i -th frame as $\sigma_i = \sigma(i, \cdot): \mathbb{Z}^+ \rightarrow \mathbb{Z}^+$, which is in fact a permutation.

We denote the j -th detection in the i -th frame as $\mathcal{D}_{ij} = \langle \mathbf{b}_{ij}, \tilde{\mathbf{c}}_{ij}, \mathbf{f}_{ij} \rangle$, and the set of detections in the i -th frame as $\mathcal{D}_i = \{\mathcal{D}_{ij} | j\}$. We refer to the k -th tracklet up to the i -th frame as a set $\mathcal{T}_{(i-1)k}$, where $\mathcal{T}_{(i-1)k}$ consists of all the detections matched to this tracklet in the previous frames, i.e., $\mathcal{T}_{(i-1)k} = \{\mathcal{D}_{i'j} | i' \leq i-1, j \leq |\mathcal{D}_{i'}|, \sigma(i', j) = k\}$. The set of tracklets up to the i -th frame is denoted as $\mathcal{T}_{i-1} = \{\mathcal{T}_{(i-1)k} | k\}$.

For each tracklet $\mathcal{T}_{(i-1)k}$, we define its position $\hat{\mathbf{b}}_{(i-1)k}$ as the bounding box of the last added detection, its class distribution and feature as the average of the distributions and features over all detections inside, i.e.,

$$\hat{\mathbf{c}}_{(i-1)k} = \frac{1}{|\mathcal{T}_{(i-1)k}|} \sum_{i' \leq i-1, j \leq |\mathcal{D}_{i'}|} \mathbb{1}_{[\sigma(i', j)=k]} \tilde{\mathbf{c}}_{i'j} \quad (8)$$

$$\hat{\mathbf{f}}_{(i-1)k} = \frac{1}{|\mathcal{T}_{(i-1)k}|} \sum_{i' \leq i-1, j \leq |\mathcal{D}_{i'}|} \mathbb{1}_{[\sigma(i', j)=k]} \mathbf{f}_{i'j}, \quad (9)$$

where $\mathbb{1}$ is the indicator function which equals to 1 if the condition holds and 0 otherwise.

A tracklet is regarded as inactive if it does not get any new detection added in the past m frames. Here, m is the number

of frames which corresponds to the time interval in the original Charades [31] videos which were annotated with scene graphs in Action Genome [15] dataset.

At the i -th frame, the detections of \mathcal{D}_i are only matched with the active tracklets in \mathcal{T}_{i-1} . We denote the number of matchings needed as n_i to assign detections \mathcal{D}_i at the i -th frame, where $n_i = \max\{|\mathcal{D}_i|, |\mathcal{T}_{i-1}|\}$. We pad with \emptyset (empty set) for detections as $\mathcal{D}'_i = \{\mathcal{D}'_{ij} | j \leq n_i, \mathcal{D}'_{ij} = \mathcal{D}_{ij} \text{ if } j \leq |\mathcal{D}_i| \text{ else } \emptyset\}$ and active tracklets as $\mathcal{T}'_{i-1} = \{\mathcal{T}'_{(i-1)j} | j \leq n_i, \mathcal{T}'_{(i-1)j} = \mathcal{T}_{(i-1)j} \text{ if } j \leq |\mathcal{T}_{i-1}| \text{ and } \mathcal{T}_{(i-1)j} \text{ is active else } \emptyset\}$.

We use the Hungarian matching algorithm [19] to assign the detections to candidate tracklets based on their class distributions, features and positions, which aims to find the permutation of n_i elements $\sigma_i \in \mathfrak{S}_{n_i}$ with the lowest cost, where \mathfrak{S}_{n_i} is the set of all permutations of size n_i :

$$\begin{aligned} \arg \min_{\sigma_i \in \mathfrak{S}_{n_i}} \mathcal{L}_{\text{Hungarian}}(\mathcal{D}'_i, \mathcal{T}'_{i-1}) = \\ \arg \min_{\sigma_i \in \mathfrak{S}_{n_i}} \sum_{j=1}^{|\mathcal{D}_i|} \mathbb{1}_{[\mathcal{T}'_{(i-1)\sigma_i(j)} \neq \emptyset]} [\mathcal{L}_{\text{dist}}(\tilde{\mathbf{c}}'_{ij}, \hat{\mathbf{c}}'_{(i-1)\sigma_i(j)}) \\ + \mathcal{L}_{\text{feat}}(\mathbf{f}'_{ij}, \hat{\mathbf{f}}'_{(i-1)\sigma_i(j)}) + \mathcal{L}_{\text{box}}(\mathbf{b}'_{ij}, \hat{\mathbf{b}}'_{(i-1)\sigma_i(j)})], \end{aligned} \quad (10)$$

where $\mathcal{L}_{\text{dist}}$, $\mathcal{L}_{\text{feat}}$ and \mathcal{L}_{box} correspond to the loss of the class distributions, features and boxes respectively.

For the class distribution and feature losses, we use the cosine cost such that

$$\mathcal{L}_{\text{dist}}(\tilde{\mathbf{c}}'_{ij}, \hat{\mathbf{c}}'_{(i-1)\sigma_i(j)}) = (1 - \cos(\tilde{\mathbf{c}}'_{ij}, \hat{\mathbf{c}}'_{(i-1)\sigma_i(j)})) \quad (11)$$

$$\mathcal{L}_{\text{feat}}(\mathbf{f}'_{ij}, \hat{\mathbf{f}}'_{(i-1)\sigma_i(j)}) = \lambda_{\text{feat}} (1 - \cos(\mathbf{f}'_{ij}, \hat{\mathbf{f}}'_{(i-1)\sigma_i(j)})), \quad (12)$$

where $\cos(\cdot, \cdot)$ represents the cosine similarity and λ_{feat} is a non-negative scalar controlling the weight between the two loss components.

Following DETR [5], we combine the L_1 loss and the generalized IoU loss [29], denoted as $\mathcal{L}_{\text{iou}}(\cdot, \cdot)$, for the box loss:

$$\mathcal{L}_{\text{box}}(\mathbf{b}'_{ij}, \hat{\mathbf{b}}'_{(i-1)\sigma_i(j)}) = \lambda_{\text{iou}} \mathcal{L}_{\text{iou}}(\mathbf{b}'_{ij}, \hat{\mathbf{b}}'_{(i-1)\sigma_i(j)}) + \lambda_{L_1} \|\mathbf{b}'_{ij} - \hat{\mathbf{b}}'_{(i-1)\sigma_i(j)}\|_1, \quad (13)$$

where λ_{iou} and λ_{L_1} control the weights of the generalized IoU loss and L_1 loss, respectively.

We create a new tracklet for an unmatched object, for example, when $\mathcal{T}'_{(i-1)\sigma_i(j)} = \emptyset$. Besides, the Hungarian matching algorithm will always assign a detection to a tracklet, nonetheless, it is not guaranteed that the detection indeed has a matching tracklet in \mathcal{T}'_{i-1} . For example, let's assume a case where the active tracklets correspond to two objects *person* and *table*; but the detections correspond to the objects *person* and *sofa*. The matching algorithm will match the *table* to *sofa*, although they are different. To mitigate this incorrect assignment problem, we ignore the matching if the cosine similarity between the features and class distributions are both less than a threshold τ . In such a case, we mark the corresponding tracklet as empty in the padded tracklet set and create a new tracklet for this detection.

Finally, the existing tracklets in \mathcal{T}_{i-1} can be updated as

$$\mathcal{T}_{ik} = \mathcal{T}_{(i-1)k} \cup \{\mathcal{D}_{ij} | \sigma_i(j) = k, \mathcal{D}'_{ij} \neq \emptyset, \mathcal{T}'_{(i-1)k} \neq \emptyset\} \quad (14)$$

Let $\mathcal{T}_0 = \emptyset$, then the tracking set could be iteratively updated and the tracking result is stored in the final tracklet set \mathcal{T}_I .

The entire coarse tracking algorithm is summarized in Algorithm 1.

Faster R-CNN usually proposes multiple bounding boxes for the same object, while our tracking algorithm assumes the unique detection for each object. Therefore, we also design a clustering algorithm that first applies Non-maximum Suppression (NMS) [28] to cluster the detections for the same object, then pass the representatives of each cluster to Algorithm 1. Finally, we assign all detections in a cluster to the tracklet that their representative belongs to. The same positional encoding for the detections in one cluster are used in the transformer encoder. More details will be available in the Supplementary material.

4.2.2 Object transformer for long-term consistency

We build a transformer on top of these tracking sequences to realize the temporal object consistency. For each detection, we represent it as a concatenation of the box embedding, class distribution embedding and object features, which can be written as

$$\mathbf{o} = \text{Concat}(g^{\text{box}}(\mathbf{b}), g^{\text{dist}}(\tilde{\mathbf{c}}), \mathbf{f}), \quad (15)$$

where g^{box} and g^{dist} stand for the embedding functions of the box and class distribution respectively, and $\mathbf{o} \in \mathbb{R}^{d_o}$.

For each tracklet, $\mathcal{T}_{Ik} = \{\mathcal{D}_{ij} | \sigma(i, j) = k\}$, we represent all of the detections inside as a matrix $\mathbf{O}_k \in \mathbb{R}^{|\mathcal{T}_{Ik}| \times d_o}$. Then we apply a three-layer transformer encoder followed by a

Algorithm 1 Coarse tracking algorithm

Input data: Detections $\mathcal{D}_1, \mathcal{D}_2, \dots, \mathcal{D}_I$ and video timestamps
Input hyperparameters: $m, \lambda_{\text{feat}}, \lambda_{\text{iou}}, \lambda_{L_1}$ and τ
 Let $\mathcal{T}_0 = \emptyset$
for iteration $i = 1, 2, \dots, I$ **do**
 Construct the padded set \mathcal{D}'_i and \mathcal{T}'_{i-1} from \mathcal{D}_i and \mathcal{T}_{i-1}
 Compute the optimal matching σ_i using Equation 10
 $k \leftarrow |\mathcal{T}_{i-1}| + 1$
 for iteration $j = 1, 2, \dots, |\mathcal{D}_i|$ **do**
 if $\mathcal{T}'_{(i-1)\sigma_j(i)} \neq \emptyset$ and $\cos(\tilde{\mathbf{c}}'_{ij}, \hat{\mathbf{c}}'_{(i-1)\sigma_i(j)}) < \tau$ and $\cos(\tilde{\mathbf{f}}'_{ij}, \hat{\mathbf{f}}'_{(i-1)\sigma_i(j)}) < \tau$ **then**
 $\mathcal{T}'_{(i-1)\sigma_i(j)} \leftarrow \emptyset$
 end if
 if $\mathcal{T}'_{(i-1)\sigma_i(j)} = \emptyset$ **then**
 Create $\mathcal{T}_{ik} \leftarrow \{\mathcal{D}_{ij}\}$ and update $k \leftarrow k + 1$
 end if
 end for
 Update the tracklets in \mathcal{T}_{i-1} according to Equation 14
 Update the tracklet set as $\mathcal{T}_i = \{\mathcal{T}_{ik} | k' = 1, 2, \dots, k-1\}$
end for
return: \mathcal{T}_I

feedforward network to output the new object class distributions $\tilde{\mathbf{C}}_k \in [0, 1]^{|\mathcal{T}_{Ik}| \times |C|}$ as:

$$\tilde{\mathbf{C}}_k = \text{Softmax}(\text{FFN}(\text{Encoder}_{\text{object}}(\mathbf{O}_k + PE(\mathbf{O}_k)))). \quad (16)$$

We can thus update the predicted class distribution for each detection in the tracklet according to $\tilde{\mathbf{C}}_k$. The regular cross entropy loss \mathcal{L}_{obj} is used for the object classification.

4.3. Temporal relationship transition

To model the relationship transition, we still ground our model on tracking sequences, but with the predicted subject-object classes, i.e., the relationships sharing the same subject-object classes¹ across the key frames are in the same sequence.

To simultaneously model the spatial dependency, we first feed all relationships into a spatial encoder, which aggregates the information in each frame, then we apply a tracking-based temporal encoder for the same subject-object pairs across frames.

The relationships are defined over a detected subject-object pair $\langle \mathcal{D}_s, \mathcal{D}_o \rangle$. Similar to STTran [6], we represent the relationships as a combination of three embeddings, visual embedding, spatial embedding and semantic embedding:

$$\mathbf{r}^{vs} = \text{Concat}(g^s(\mathbf{f}_s), g^o(\mathbf{f}_o)) \quad (17)$$

$$\mathbf{r}^{sp} = g^{sp}(\mathbf{u}_{so} \oplus g^{\text{boxes}}(\mathbf{b}_s, \mathbf{b}_o)) \quad (18)$$

$$\mathbf{r}^{se} = \text{Concat}(g^{se}(\mathbf{c}_s), g^{se}(\mathbf{c}_o)) \quad (19)$$

$$\mathbf{r} = \text{Concat}(\mathbf{r}^{vs}, \mathbf{r}^{sp}, \mathbf{r}^{se}), \quad (20)$$

¹In Action Genome [15], each object class is unique in one frame.

where \mathbf{r}^{vs} , \mathbf{r}^{sp} , \mathbf{r}^{se} correspond to the visual embedding, spatial embedding and semantic embedding, respectively. g^s and g^o are the visual feature embedding functions for the subject and object. g^{sp} is the spatial embedding function, whose input is the sum of the union feature \mathbf{u}_{so} for the subject and object extracted by ROIALign [11] and a boxes embedding encoded by g^{boxes} , where \oplus stands for the element-wise addition. g^{se} is the word embedding of the object class. We refer more details about each embedding function to the Supplementary material.

Let the relationship matrix inside i -th frame be denoted as \mathbf{R}_i for $i=1,2,\dots,I$. The output of the spatial encoder is:

$$\mathbf{R}'_i = \text{Encoder}_{\text{spatial}}(\mathbf{R}_i). \quad (21)$$

Here we use a one-layer transformer encoder with no positional encoding, since the order of the detections inside one frame does not matter.

Then we rearrange all \mathbf{R}'_i according to their subject and object classes, which we write \mathbf{R}'_{so} for the relationship matrix of subject-object classes $\langle s, o \rangle$, then the logits of the predicates can be calculated as

$$\mathbf{Z}_{so} = \text{Encoder}_{\text{temporal}}(\mathbf{R}'_{so} + PE(\mathbf{R}'_{so})). \quad (22)$$

And we use a three-layer transformer encoder, similar to the object encoder, on the predicted subject-object classes sequences.

The predicates logits \mathbf{z} of each subject-object pair in a frame will go through different linear projections to obtain the final predicates distribution $\tilde{\mathbf{p}}$ for different HOI types belonging to *attention*, *spatial* and *contact* as defined in the Action Genome dataset [15]. We use the multi-label margin loss for the predicate classification,

$$\mathcal{L}_p(\tilde{\mathbf{p}}) = \sum_{i \in \mathcal{P}^+} \sum_{j \in \mathcal{P}^-} \max(0, 1 - \tilde{\mathbf{p}}[j] + \tilde{\mathbf{p}}[i]), \quad (23)$$

where \mathcal{P}^+ denotes the indices of the annotated predicates and \mathcal{P}^- denotes the indices of the predicates not in the annotation.

The final loss combines both the object loss and predicate loss $\mathcal{L}_{\text{total}} = \mathcal{L}_{\text{obj}} + \mathcal{L}_p$.

5. Experiments

In this section, we conduct the empirical evaluations to answer the following research questions (RQ): **RQ1** How does the proposed method exploit long-term dependencies via tracking, compare with previous video SGG methods? **RQ2** What is the best extent possible to exploit long-term dependencies for dynamic SGG tasks? **RQ3** How does each module in our method contribute to the performance on the dynamic SGG tasks?

5.1. Experimental setup

Dataset We evaluate our method on Action Genome dataset [15] containing 35 object categories and 25 relationship

categories. The relationships are categorized into three human-object categories: attention, spatial and contact relationships, where multiple relationships may appear in spatial and contact categories.

Training We use one NVIDIA Tesla V100S GPU with 32G memory for training. Similar to [6], we utilize Faster R-CNN with Resnet101 [12] backbone for the object detector and pre-train it on Action Genome [15]. All layers in the backbone for the object detector feature extraction are frozen when training our method. We use AdamW [23] to optimize with batch size 1. The initial learning rate is set to 10^{-5} .

Evaluation There are three different scene graph generation tasks in increasing level of difficulty, namely: (1) predicate classification (PredCls): The task is to predict the predicates of the relationship tuples, given the video frames, ground truth bounding boxes and object labels. (2) scene graph classification (SGCls): where the video frames and bounding boxes are provided and the task is to predict the predicates and subject/object classes. (3) scene graph detection (SGDet): The task is to detect the objects and predict the predicates for object pairs, where only the video frames are provided. Following the convention of object detection, in case of SGDet, an entity (subject or object) is regarded as successfully detected if the Intersection-Over-Union (IOU) between the predicted bounding box and the ground truth bounding box is larger than 0.5 and the predicted and ground-truth class labels match.

For the SGG tasks, we use Recall@K (R@K, $K=[10,20,50]$) [24, 15] as the evaluation metric, which measures the fraction of the ground-truth relationship triplets in the top K predictions. There are two main ways for the R@K calculation, **With Constraint** and **No Constraint**. **With Constraint** is a strict evaluation strategy that constrains the model to predict only one relationship for a subject-object pair, thus requiring it to detect the most important relationships. In contrast, **No Constraint** allows the model to make multiple predictions for any subject-object pair, which is suitable for the multi-label evaluation, such as the contact relationships in Action Genome. We use the R@K with constraint as the primary evaluation metric, and report the results of the model with the highest R@K with constraint score.

For the relationship tuple of a subject-object pair $\langle \mathcal{D}_s, \mathcal{D}_o \rangle$, we define the score of each detected object as the highest class score in its distribution, $\max\{\tilde{\mathbf{c}}\}$. Then the score of i -th relationship triplet is estimated as the product of three scores:

$$\max\{\tilde{\mathbf{c}}_s\} \cdot \tilde{\mathbf{p}}[i] \cdot \max\{\tilde{\mathbf{c}}_o\}. \quad (24)$$

For the calculation of R@K, the relationship triplets are ordered according to their scores among all relationship triplets of that category in a frame.

Table 1: Comparison with state-of-the-art scene graph generation methods on Action Genome [15]. The same object detector is used in all baselines for fair comparison. † denotes reproduced results via STTran’s [6] source code [1] which DSG-DETR is built atop.

Method	With Constraint									No Constraints								
	PredCls			SGCls			SGDet			PredCls			SGCls			SGDet		
	R@10	R@20	R@50	R@10	R@20	R@50	R@10	R@20	R@50	R@10	R@20	R@50	R@10	R@20	R@50	R@10	R@20	R@50
VRD [24]	51.7	54.7	54.7	32.4	33.3	33.3	19.2	24.5	26.0	59.6	78.5	99.2	39.2	49.8	52.6	19.1	28.8	40.5
M-FREQ [40]	62.4	65.1	65.1	40.8	41.9	41.9	23.7	31.4	33.3	73.4	92.4	99.6	50.4	60.6	64.2	22.8	34.3	46.4
MSDN [21]	65.5	68.5	68.5	43.9	45.1	45.1	24.1	32.4	34.5	74.9	92.7	99.0	51.2	61.8	65.0	23.1	34.7	46.5
VCtree [33]	66.0	69.3	69.3	44.1	45.3	45.3	24.4	32.6	34.7	75.5	92.9	99.3	52.4	62.0	65.1	23.9	35.3	46.8
ReIDN [41]	66.3	69.5	69.5	44.3	45.4	45.4	24.5	32.8	34.9	75.7	93.0	99.0	52.9	62.4	65.1	24.1	35.4	46.8
GBS-Net [22]	66.8	69.9	69.9	45.3	46.5	46.5	24.7	33.1	35.1	76.0	93.6	99.5	53.6	63.3	66.0	24.4	35.7	47.3
STTran [6]	68.6	71.8	71.8	46.4	47.5	47.5	25.2	34.1	37.0	77.9	94.2	99.1	54.0	63.7	66.4	24.6	36.2	48.8
Baseline(STTran [6])†	68.1	71.2	71.2	45.7	46.8	46.8	25.1	33.9	36.8	78.7	94.4	99.2	54.2	63.5	66.0	24.6	36.2	48.9
DSG-DETR(Ours)	68.5	71.7	71.7	50.4	51.6	51.6	30.0	34.4	35.6	78.3	94.2	99.1	59.5	69.4	72.4	31.5	40.5	48.3

5.2. Comparison with SOTA (RQ1)

Table 1 shows the main result of the proposed DSG-DETR. We use the state-of-the-art dynamic scene graph generation method called STTran [6] as our strongest baseline, and develop our DSG-DETR atop their source code [1]. Besides, we also select some powerful scene graph generation methods on the static images such as VRD [24], M-FREQ [40], MSDN [33], ReIDN [41] and GBS-Net [22]. For fair comparison, we use the same object detector, a pretrained Faster R-CNN fine-tuned on Action Genome for all the baselines. The results show that DSG-DETR outperforms the strongest baseline of STTran in both SGClS and SGDet tasks where long-term dependencies are essential for consistent object recognition. DSG-DETR clearly outperforms the state-of-art by $\sim 8\%$ - 10% and $\sim 19\%$ - 28% in terms of R@10 under constraint and no constraint criteria for SGClS and SGDet, respectively. PredCls task, on the other hand, is almost saturated since the ground truth object classes and their locations both are given as input. Please note that for the PredCls model, the only difference between our DSG-DETR and STTran baseline lies in the relationship transformer, where DSG-DETR exploits the tracking sequences and DSG-DETR yields $\sim 0.5\%$ improvement over our baseline on R@10 metric under the Constrained criteria. Given the ground truth object locations and classes as input, even this small improvement suggests the importance of our tracking-based sequence construction for capturing the long-term temporal context for visual relationships.

We observe that the improvement of DSG-DETR becomes minor when it comes to larger K for SGDET, this is in fact a tradeoff between the consistency and the diversity, however, we believe the consistency is a more important characteristics of human perception even for wrong predictions.

5.3. Best case: with ground-truth tracks (RQ2)

To address RQ2, we first construct the sequences based on the ground truth object classes. Such sequences can be treated as the hypothetical *best case* to exploit the long-term dependencies. We see in Table 2 that the *best case* scenario of exploiting the long-term dependencies largely improves the performance

Table 2: Hypothetical *best case* when exploiting long-term dependencies. GTTrack includes all components of DSG-DETR but uses the ground truth object tracks instead. DSG-DETR relies on coarse object tracking, outperforms the baseline and performs comparably with GTTrack.

Method	With Constraint				No Constraints			
	SGClS		SGDet		SGClS		SGDet	
	R@10	R@20	R@10	R@20	R@10	R@20	R@10	R@20
Baseline(STTran [1])	45.7	46.8	25.2	34.1	54.2	63.5	24.6	36.2
GTTrack (Upper-bound)	52.6	53.8	36.6	37.6	62.0	71.6	43.7	50.3
DSG-DETR(Ours)	50.4	51.6	30.0	34.4	59.5	69.4	31.5	40.5

over the baseline; Specifically, SGClS improves by $\sim 13\%$ - 14% and SGDet improves by $\sim 45\%$ - 46% over the baseline. We also demonstrate that our proposed tracking algorithm helps in reducing the gap between DSG-DETR and the ground-truth tracklet upper-bound in all cases. For example, the *best case* for SGClS performs only $\sim 4\%$ better than DSG-DETR in terms of R@10. For SGDet, DSG-DETR is able to reduce the performance gap from the *best case* by almost half comparing with the baseline ($\sim 45\%$ vs $\sim 21\%$) in terms of R@10.

5.4. Ablation studies (RQ3)

In DSG-DETR, we propose to capture long-term dependencies primarily by consistent and effective object tracklets construction. We employ two transformers - one for consistent object prediction and the other for relationship transitions. For the object transformer, we additionally integrate the temporal position with the object representations into the transformer encoder through positional encoding, denoted by “Pos enc” in the ablation table 3. Our relationship transformer architecture shares the same spatial encoder as STTran [6], but it replaces the temporal decoder in STTran with a temporal encoder operating on the predicted classes sequences for capturing the long-term dependencies. In table 3, we replace our relationship transformer with STTran for ablation. We show the results of ablating our model for SGClS task.

The heavy lifting is done by the object transformer employed

Table 3: Ablation experiments for SGCLs. The first row denotes the reproduced results of STTran, with its relationship transformer.

Obj trans	Pos enc	Rela trans	With Constraint			No Constraint		
			R@10	R@20	R@50	R@10	R@20	R@50
-	-	-	45.7	46.8	46.8	54.2	63.5	66.0
-	-	✓	46.0	47.1	47.1	54.6	63.5	65.9
✓	-	✓	50.2	51.4	51.4	58.1	68.7	71.9
✓	✓	✓	50.4	51.6	51.6	59.5	69.4	72.4

on the constructed tracklets. For relationship transformer, the first two rows in the table demonstrate that even with the predicted classes sequences based on Faster R-CNN results, capturing the long-term dependencies still brings the benefits with 0.3 point improvement compared with STTran in R@K under constraint. Finally, the positional encoding in the object transformer boosts the performance by additional 0.2 point in terms of R@K under constraint and even significant improvement for no constraint evaluation. The ablative studies for SGGDet also exhibits similar trend, and available in the Supplementary material.

5.5. Qualitative results

Fig 3 is an example where DSG-DETR successfully constructs the sequence of the blue bowl (Figs 3(a) and 3(b)) from the temporally ordered key frames (top to bottom) and makes the correct prediction “dish” for all of them. While Faster R-CNN and STTran will mis-classify as shown in Fig 3(c).

Fig 4 shows an example frame where DSG-DETR constructed a tracklet of a blanket shown in the red bounding box. Most of the detections in the tracklet are predicted as “person” by Faster R-CNN shown in Fig 4 (b). However, the object transformer makes a correct prediction “blanket” for all of them in the sequence. This reveals that the object transformer in fact learns to reason over temporal dependencies beyond a simple majority voting.

In Fig 5, we sample three key frames for an action where a person gets up from the bed and walks towards the doorway. The first frame is 33 frames away from the third one in the original video. Thanks to its capability to exploit long-term dependencies, DSG-DETR successfully understands the whole action with only one mistake which is mis-classifying “touching” as “sitting on” in the first frame. However, STTran makes many mistakes including predicting that the human is still “sitting on” the bed in the second frame and the bed is “on the side of” the human in the third frame rather than “behind”.

6. Discussions

Limitations and Future Work. The performance gap between the hypothetical *best case* or the upper-bound and DSG-DETR shows that there is still room to improve the tracklet construction. We also tried several off-the-shelf object tracker for the tracklet construction process, they turned out to be sub-par for SGG tasks possibly due to their inability to automatically



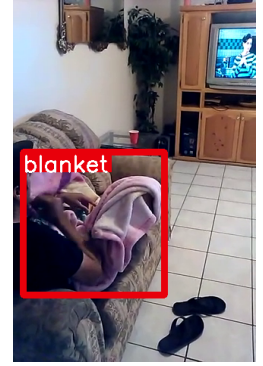
(a) Correctly classified by all models.



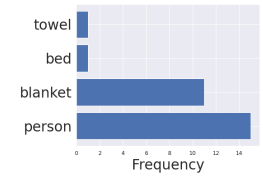
(b) Correctly classified by DSG-DETR.



(c) Mis-classified by STTran and Faster R-CNN.



(a) “Blanket” (in red box).



(b) Histogram of Faster R-CNN predictions on the “blanket” objects in the tracklet.

Figure 4: DSG-DETR recovers from the Faster R-CNN classification error in the tracklet.

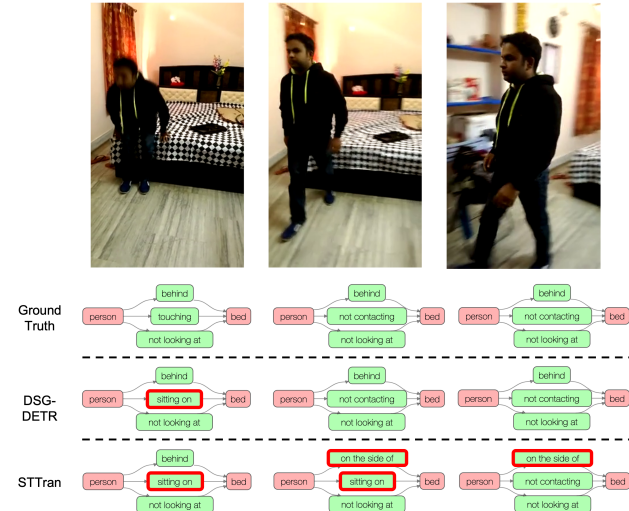


Figure 5: Scene graphs generated by DSG-DETR and STTran for three key frames sampled from an action which embeds long-term dependencies.

reinitialize in case of sudden object appearance or disappearance.

Conclusions. We hypothesized that capturing long-term temporal context is crucial for dynamic scene graph generation. To this end, we estimated an upper-bound on the performance of SGG tasks by utilizing ground truth object tracks. We also presented a framework called Dynamic Scene Graph Detection Transformer (DSG-DETR) that is capable of exploiting long-term dependencies by coarse tracking without access to ground truth object tracks. In DSG-DETR, we proposed to construct long-term and effective object-level tracklets to capture object dynamics via the detect-track-recognize paradigm and to model the relationship transitions on the predicted subject-object classes sequences. We showed that both transformers capture the long-term context effectively when applied on those constructed sequences, and showed that DSG-DETR notably closes the performance gap between the baseline and the upper-bound. We demonstrated the efficacy of DSG-DETR on the Action Genome dataset, where it significantly outperforms the state-of-the-art methods.

References

- [1] Spatial-temporal transformer for dynamic scene graph generation. [https://urldefense.com/v3/_https://github.com/yrcong/STTran_!!DZ3fjg!pJWVI_1fz7dASo2_ebhTPZLLuiY8djm_QiuWaxTjEE4cYQCbacknJ9T8dJ6CvdwuY9dY\\$](https://urldefense.com/v3/_https://github.com/yrcong/STTran_!!DZ3fjg!pJWVI_1fz7dASo2_ebhTPZLLuiY8djm_QiuWaxTjEE4cYQCbacknJ9T8dJ6CvdwuY9dY$.). Accessed: 2021-08-30.
- [2] Peter Anderson, Basura Fernando, Mark Johnson, and Stephen Gould. Spice: Semantic propositional image caption evaluation, 2016.
- [3] Anurag Arnab, Chen Sun, and Cordelia Schmid. Unified Graph Structured Models for Video Understanding. *arXiv:2103.15662 [cs]*, Mar. 2021.
- [4] Nicolas Carion, Francisco Massa, Gabriel Synnaeve, Nicolas Usunier, Alexander Kirillov, and Sergey Zagoruyko. End-to-end object detection with transformers. In Andrea Vedaldi, Horst Bischof, Thomas Brox, and Jan-Michael Frahm, editors, *Computer Vision - ECCV 2020 - 16th European Conference, Glasgow, UK, August 23-28, 2020, Proceedings, Part I*, volume 12346 of *Lecture Notes in Computer Science*, pages 213–229. Springer, 2020.
- [5] Nicolas Carion, Francisco Massa, Gabriel Synnaeve, Nicolas Usunier, Alexander Kirillov, and Sergey Zagoruyko. End-to-end object detection with transformers, 2020.
- [6] Yuren Cong, Wentong Liao, Hanno Ackermann, Bodo Rosenhahn, and Michael Ying Yang. Spatial-Temporal Transformer for Dynamic Scene Graph Generation. In *Proceedings of the International Conference on Computer Vision (ICCV)*, October 2021.
- [7] Alexey Dosovitskiy, Lucas Beyer, Alexander Kolesnikov, Dirk Weissenborn, Xiaohua Zhai, Thomas Unterthiner, Mostafa Dehghani, Matthias Minderer, Georg Heigold, Sylvain Gelly, Jakob Uszkoreit, and Neil Houlsby. An image is worth 16x16 words: Transformers for image recognition at scale. *ICLR*, 2021.
- [8] Noa Garcia and Yuta Nakashima. Knowledge-based video question answering with unsupervised scene descriptions. In *ECCV (18)*, volume 12363 of *Lecture Notes in Computer Science*, pages 581–598. Springer, 2020.
- [9] Rohit Girdhar, João Carreira, Carl Doersch, and Andrew Zisserman. Video action transformer network. In *CVPR*, pages 244–253. Computer Vision Foundation / IEEE, 2019.
- [10] Jiawei He, Zehao Huang, Naiyan Wang, and Zhaoxiang Zhang. Learnable graph matching: Incorporating graph partitioning with deep feature learning for multiple object tracking. In *Proceedings of the IEEE/CVF Conference on Computer Vision and Pattern Recognition (CVPR)*, pages 5299–5309, June 2021.
- [11] Kaiming He, Georgia Gkioxari, Piotr Dollár, and Ross Girshick. Mask r-cnn, 2018.
- [12] Kaiming He, Xiangyu Zhang, Shaoqing Ren, and Jian Sun. Deep residual learning for image recognition, 2015.
- [13] Drew A. Hudson and Christopher D. Manning. GQA: A new dataset for real-world visual reasoning and compositional question answering. In *The IEEE Conference on Computer Vision and Pattern Recognition (CVPR)*, June 2019.
- [14] Jingwei Ji, Rishi Desai, and Juan Carlos Nibbles. Detecting human-object relationships in videos. In *Proceedings of the International Conference on Computer Vision (ICCV)*, October 2021.
- [15] Jingwei Ji, Ranjay Krishna, Li Fei-Fei, and Juan Carlos Nibbles. Action Genome: Actions as Composition of Spatio-temporal Scene Graphs. In *Proceedings of the IEEE/CVF Conference on Computer Vision and Pattern Recognition (CVPR)*, June 2020.
- [16] Justin Johnson, Agrim Gupta, and Li Fei-Fei. Image generation from scene graphs, 2018.
- [17] Justin Johnson, Ranjay Krishna, Michael Stark, Li-Jia Li, David A. Shamma, Michael S. Bernstein, and Li Fei-Fei. Image retrieval using scene graphs. In *2015 IEEE Conference on Computer Vision and Pattern Recognition (CVPR)*, pages 3668–3678, 2015.
- [18] Ranjay Krishna, Yuke Zhu, Oliver Groth, Justin Johnson, Kenji Hata, Joshua Kravitz, Stephanie Chen, Yannis Kalantidis, Li-Jia Li, David A. Shamma, Michael S. Bernstein, and Li Fei-Fei. Visual genome: Connecting language and vision using crowdsourced dense image annotations. *Int. J. Comput. Vision*, 123(1):32–73, May 2017.
- [19] H. W. Kuhn and Bryn Yaw. The hungarian method for the assignment problem. *Naval Res. Logist. Quart.*, pages 83–97, 1955.
- [20] Yikang Li, Tao Ma, Yeqi Bai, Nan Duan, Sining Wei, and Xiaogang Wang. Pastegan: A semi-parametric method to generate image from scene graph. In *Advances in Neural Information Processing Systems 32: Annual Conference on Neural Information Processing Systems 2019, NeurIPS 2019, 8-14, December 2019, Vancouver, BC, Canada*, pages 3950–3960, 2019.
- [21] Yikang Li, Wanli Ouyang, Bolei Zhou, Kun Wang, and Xiaogang Wang. Scene graph generation from objects, phrases and region captions. *2017 IEEE International Conference on Computer Vision (ICCV)*, pages 1270–1279, 2017.
- [22] Xin Lin, Changxing Ding, Jinqian Zeng, and Dacheng Tao. Gps-net: Graph property sensing network for scene graph generation. In *Proc. IEEE Conf. Comput. Vis. Pattern Recognit.*, pages 3746–3753, 2020.
- [23] Ilya Loshchilov and Frank Hutter. Decoupled weight decay regularization, 2019.

- [24] Cewu Lu, Ranjay Krishna, Michael Bernstein, and Li Fei-Fei. Visual relationship detection with language priors. In *European Conference on Computer Vision*, 2016.
- [25] Kien Nguyen, Subarna Tripathi, Bang Du, Tanaya Guha, and Truong Q. Nguyen. In defense of scene graphs for image captioning. In *Proceedings of the IEEE/CVF International Conference on Computer Vision (ICCV)*, pages 1407–1416, October 2021.
- [26] Son T. Nguyen, Ozgur S. Oguz, Valentin N. Hartmann, and Marc Toussaint. Self-supervised learning of scene-graph representations for robotic sequential manipulation planning. In *4rd Annual Conference on Robot Learning, CoRL 2020, Proceedings, Proceedings of Machine Learning Research*. PMLR, 2020.
- [27] Niki Parmar, Ashish Vaswani, Jakob Uszkoreit, Lukasz Kaiser, Noam Shazeer, Alexander Ku, and Dustin Tran. Image transformer. In Jennifer Dy and Andreas Krause, editors, *Proceedings of the 35th International Conference on Machine Learning*, volume 80 of *Proceedings of Machine Learning Research*, pages 4055–4064. PMLR, 10–15 Jul 2018.
- [28] Shaoqing Ren, Kaiming He, Ross Girshick, and Jian Sun. Faster r-cnn: Towards real-time object detection with region proposal networks, 2016.
- [29] Hamid Rezatofighi, Nathan Tsoi, JunYoung Gwak, Amir Sadeghian, Ian Reid, and Silvio Savarese. Generalized intersection over union. In *The IEEE Conference on Computer Vision and Pattern Recognition (CVPR)*, June 2019.
- [30] Sebastian Schuster, Ranjay Krishna, Angel Chang, Li Fei-Fei, and Christopher D. Manning. Generating semantically precise scene graphs from textual descriptions for improved image retrieval. In *Proceedings of the Fourth Workshop on Vision and Language*, pages 70–80, Lisbon, Portugal, Sept. 2015. Association for Computational Linguistics.
- [31] Gunnar A. Sigurdsson, Gül Varol, Xiaolong Wang, Ali Farhadi, Ivan Laptev, and Abhinav Gupta. Hollywood in homes: Crowdsourcing data collection for activity understanding, 2016.
- [32] Chen Sun, Austin Myers, Carl Vondrick, Kevin Murphy, and Cordelia Schmid. Videobert: A joint model for video and language representation learning. In *Proceedings of the IEEE/CVF International Conference on Computer Vision (ICCV)*, October 2019.
- [33] Kaihua Tang, Hanwang Zhang, Baoyuan Wu, Wenhan Luo, and Wei Liu. Learning to compose dynamic tree structures for visual contexts. In *The IEEE Conference on Computer Vision and Pattern Recognition (CVPR)*, June 2019.
- [34] Yao Teng, Limin Wang, Zhifeng Li, and Gangshan Wu. Target Adaptive Context Aggregation for Video Scene Graph Generation. In *Proceedings of the International Conference on Computer Vision (ICCV)*, October 2021.
- [35] Hung-Yu Tseng, Hsin ying Lee, Lu Jiang, Ming-Hsuan Yang, and Weilong Yang. RetrieveGAN: Image synthesis via differentiable patch retrieval. In *ECCV*, 2020.
- [36] Ashish Vaswani, Noam Shazeer, Niki Parmar, Jakob Uszkoreit, Llion Jones, Aidan N Gomez, Łukasz Kaiser, and Illia Polosukhin. Attention is all you need. In I. Guyon, U. V. Luxburg, S. Bengio, H. Wallach, R. Fergus, S. Vishwanathan, and R. Garnett, editors, *Advances in Neural Information Processing Systems*, volume 30. Curran Associates, Inc., 2017.
- [37] Sijin Wang, Ruiping Wang, Ziwei Yao, Shiguang Shan, and Xilin Chen. Cross-modal scene graph matching for relationship-aware image-text retrieval. In *IEEE Winter Conference on Applications of Computer Vision, WACV 2020, Snowmass Village, CO, USA, March 1-5, 2020*, pages 1497–1506. IEEE, 2020.
- [38] Xu Yang, Kaihua Tang, Hanwang Zhang, and Jianfei Cai. Auto-encoding scene graphs for image captioning. In *The IEEE Conference on Computer Vision and Pattern Recognition (CVPR)*, June 2019.
- [39] Ting Yao, Yingwei Pan, Yehao Li, and Tao Mei. Exploring visual relationship for image captioning. In *The European Conference on Computer Vision (ECCV)*, September 2018.
- [40] Rowan Zellers, Mark Yatskar, Sam Thomson, and Yejin Choi. Neural motifs: Scene graph parsing with global context. *CoRR*, abs/1711.06640, 2017.
- [41] Ji Zhang, Kevin J. Shih, Ahmed Elgammal, Andrew Tao, and Bryan Catanzaro. Graphical contrastive losses for scene graph parsing. In *CVPR*, 2019.